Simulating the Performance of $Al_xGa_{1-x}As$/InP/Ge MJSC Under Variation of SI and Temperature

Giriraj Sahu, Kusum Dewangan, Soumya John, Aloke Verma*

[1] Department of Physics, Kalinga University, Naya Raipur (C.G.) India 492101

* Corresponding Author Email Id: alokeverma1785@gmail.com;

DOI:10.48047/ecb/2023.12.si4.710

Abstract

Mechanically stacked $Al_xGa_{1-x}As$/InP/Ge MJSC' sensitivity to SI and temperature variations was simulated. MATLAB code was using to the system received and spectra transmitting of separately z-matrix, while PC1D code modelled the energy generation. Multiplying the AM1.5d spectrum by values of SIMF (1- 200 suns) yielded the ISR on the foremost z-matrix. Temperatures of 25- 100 °C were used in each simulation run. In contrast to the stochastic response of the SCEs brought about by the SIMF changes, the simulation findings show that the V_{OC} and efficiency of the SCs behave linearly changes in temperature. The results of the simulations also show that the optimal performance is achieved with an irradiance spectrum exposure of 100 suns and a functional temperature of 25 °C.

Keywords: MJSC (Multijunction solar cell), AM1.5d spectrum, MATLAB, SIFM, PC1D, SI (spectral irradiance).

1. Introduction

Formerly two decades, researchers have made major progress in the study of SCs and PVCs. There has been a lot of study into silicon-based, CIGS-based, and III-V-based materials with the ultimate objective of developing a HESCs. Many sources have brought consideration to the worldwide effort to perfect a solar cell that will provide reliable, long-term power. Here, the grouping of III-V based SCs materials including GIP, AGA, IP, and GA in MJSCs and exposure to several hundred multiplications of SRs, the GIP/GA/GIAP/GIA system had an efficiency rate of 46% at 508 suns [1]. Improvements in SCs technology include a six-junction cell, LSCs, and a straight up architecture of epitaxial heterostructure [2]. High-efficiency MJSC tests have primarily been conducted on a prototype's size, and their commercial and industrial implementation is still in the future. It is crucial to model and

simulate MJSC in a variety of settings. The p-n junctions of the semiconducting layers (or z-matrixs) in a MJSCs are arranged in descending order of bandgap energy. The foremost layer absorbs SRs in the short-wavelength region due to its high bandgap energy, whereas the subsequent layers do so in the longer-wavelength range [3]. Adding more z-matrixs to a solar cell should, in theory, boost its efficiency. MJSCs can be made in two distinct ways: monolithically integrated or mechanically stacked. The matching of electric current and lattice, and tunnel junction between z-matrixs of MJSC are the limiting factors in MJSC efficiency. All of these problems disappear when mechanically stacked MJSC are subjected to z-matrix-specific load regulation. A see-through middle ground between

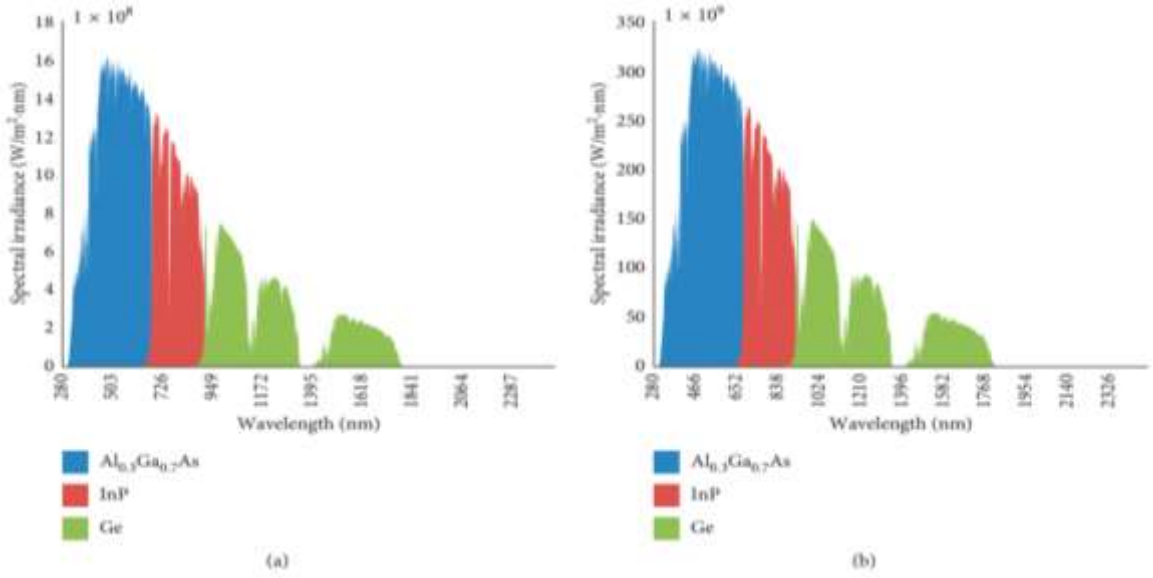

Figure 1. Absorption ranges of individual z-matrixs as well as the incoming AM1.5d spectra for (a) SIMF 1 (one sun) and (b) SIMF 200 (more than two hundred suns).

optical losses in mechanically stacked MJSC can be minimised by placing a conductive layer like ITO between two adjacent z-matrixs [4, 5]. Neither experimental nor computational studies of MJSCs efficiency have examined the $Al_xGa_{1-x}As$/InP/Ge SCs under temperature and intense radiation. In this study, PC1D is used to model the behaviour of $Al_xGa_{1-x}As$/InP/Ge MJSCs subject to varying temperatures and irradiance spectra (produced by concentrators). The author is unaware of any attempts to model the effects of MJSC using the PC1D software. This research could pave the way to a solar cell that is reliable, long-lasting, and highly effective [6].

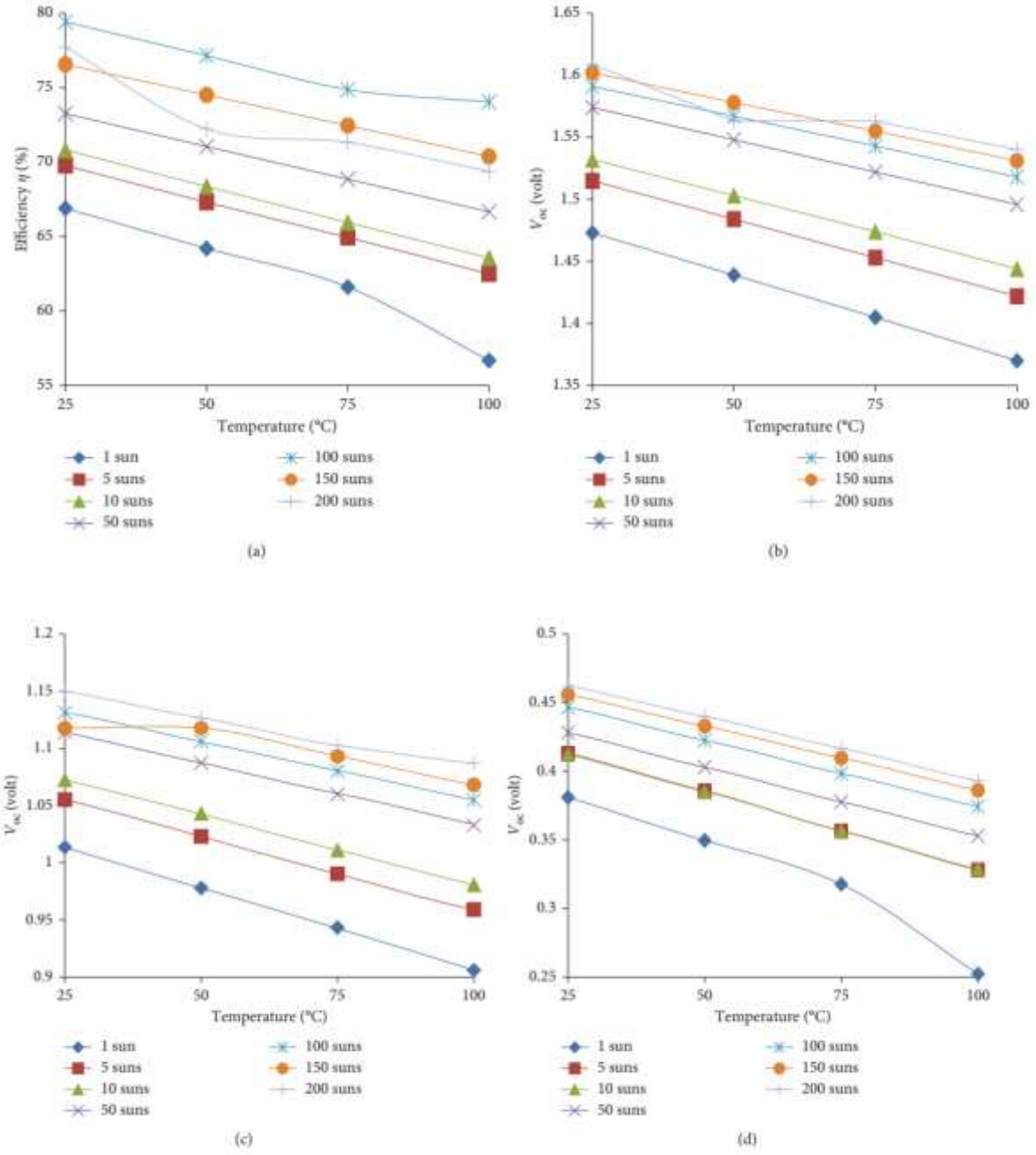

Figure 2. $Al_xGa_{1-x}As$/InP/Ge multijunction solar cell (a) efficiency as a function of temperature. What happens to the open-circuit voltage of (b) $Al_xGa_{1-x}As$, (c) InP, and (d) Ge when the temperature changes.

2. Method

The three phases involved in this investigation include preparing the incoming spectrum, conniving the $\alpha(\lambda)$ and transmitted radiation, and modelling power generation [7]. The incidence SI on the first z-matrix was computed for 5 to 200 suns using the AM1.5d direct

solar spectrum (ASTM G173-03) for one sun's radiation. To rebuild the smoothed AM1.5d SI, the constant $b(\lambda)$ was computed using a blackbody radiation formula. Using the PC1D software, we were able to determine the thickness of the nth cell, and then multiply that value by the total incoming radiation [8]. The electrical efficiency of the MJSC was simulated by measuring the I_{SC}, V_{OC}, P_n, and the P_0. The spectrum irradiance, or wavelength dependence, of blackbody radiation at the earth's surface (earthly) is given as follows [9-12].

$$I_1(\lambda, T) = \frac{2\pi hc^2}{\lambda^5} \exp\left[\frac{\lambda k_B T}{hcb(\lambda)}\right] \left(\frac{r_{sun}}{R}\right)^2$$

……. (1)

where r_{sun} represents the radius of sun, R represents the distance between the sun's centre and Earth's surface, h represents the Planck constant, and k_B represents the Boltzmann constant [13]. The value of $b(\lambda)$ is obtained by integrating the full spectrum using a trapezoid approach and fixing the intensity to 990 W/m^2. This allows us to restructure the smoothed AM1.5d spectrum through interpolation [14-16].

The $\alpha(\lambda)$ of each z-matrix was calculated using Equation (2) following the reference:

$$\alpha(\lambda) = 5.5\sqrt{E(\lambda) - E_g} + 1.5\sqrt{E(\lambda) - \left(E_g + 0.1\right)}\, \mu m^{-1}$$

…… (2)

where $E(\lambda)$ is the energy of an incident photon of that wavelength, E_g is the bandgap energy of the consistent z-matrix, and $\alpha(\lambda)$ is the absorption coefficient as a function of wavelength [17].

Intensity transmitted to z-matrix I_{n+1} is a function of solar energy received in z-matrix I_n, z-matrix d_n thickness, and z-matrix $\alpha_n(\lambda)$ absorption coefficient, $I_n(\lambda)$ as shown below

$$I_n(\lambda) = I_{n-1}(\lambda) \exp[-\alpha_n(\lambda) d_n]$$

$n = 1, 2, 3$, for triple junction solar cell [18].

…… (3)

where I_0 is the SI entering the first z-matrix, I_1 the SI entering the second, and I_2 the SI entering the third [19]. The PC1D software was used to determine the thickness of the

n^{th} cell, denoted by the symbol d_n [20]. Depending on the number of junctions involved, it may be necessary to conduct a large number of simulations in order to overcome the program's limits [21].

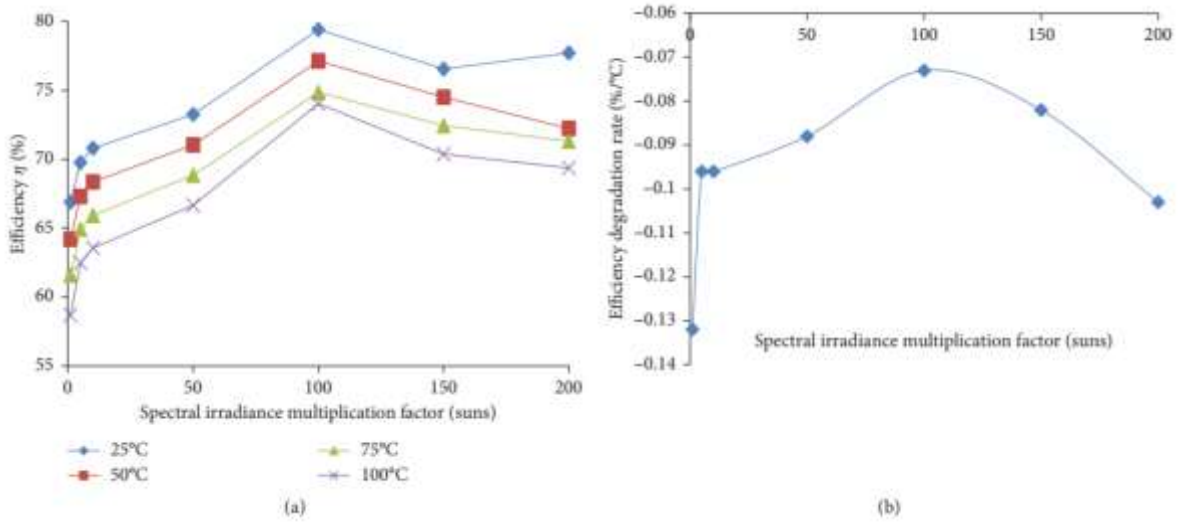

Figure 3. Multiplication of spectrum irradiance and its impact on (a) solar cell overall efficiency and (b) SCEs deterioration rate.

The following equation is then used to get the total amount of incoming radiation after multiplication [22].

$$I_{mul} = I_0 \times SIMF$$

…… (4)

where I_{mul} is the spectrum irradiance after being multiplied by a factor of SIMF that was varied between 1 to 200 suns [23-25]. Here, simulated the electrical efficiency of the MJSC by measuring its short circuit current (I_{SC}), open circuit voltage (V_{OC}), output power (P_n), and total efficiency (η) for each set of simulations [26]. The following equation is then used to get the overall efficiency of the mechanically stacked MJSC.

$$\eta = \frac{P_1 + P_2 + P_3}{P_0}$$

……. (5)

The MJSC can play out two hypothetical situations: with and without symmetry, the current through each z-matrix is balanced out, and a nonidentical electric current model optimizes

output power in each z-matrix and overall efficiency [27]. The current, nonidentical model is expected to achieve efficiency of greater than 70%, compared to the MJSC's previous efficiency of 45%. This modelling can be seen as a toy model due to simplifications and idealizations, and issues such as hotspot formation, current mismatch across z-matrixs, and an increase in resistive losses are not taken into account [28].

Table 1 The efficiency enhancement at various temperatures and SIMF's ranges.

Temperature (°C)	Efficiency improvement within SIMF's range of 1 to 100 suns (%).	Gains in productivity (%) within the 100-200-sun range of SIMF.
25	19.01	– 2.15
50	20.20	– 6.40
75	21.60	– 5.00
100	30.57	– 6.30

3. Results and Discussions

Using Eqs. (1) and (3), we determined the MJSC's maximum SI and intensity. Solar concentrators increase the temperature and improve the light absorption of MJSC solar cells [17, 24]. The MJSC's overall efficiency rose nonlinearly with increasing SIMF, reaching a maximum at around 100 SI before gradually declining to a condition of saturation [1-4]. SCEs decreases from -0.13%/°C to -0.07%/°C when the SIMF grows from 1 to 100 suns, and then increases to -0.10%/°C at 200 suns, mirroring the stochastic response of MJSC to change in SIMF [23]. The figure displays the current-voltage (I-V) characteristic of each z-matrix at 25°C and 75°C, and for SIMFs of 50 to 200 suns [25]. Using Eqs. (1) and (3), we determined the MJSC's maximum SI and intensity.

Solar concentrators increase the temperature and improve the light absorption of MJSC solar cells [6, 17]. The MJSC's overall efficiency rose nonlinearly with increasing SIMF, reaching a maximum at around 100 SI before gradually declining to a condition of saturation. SCEs decreases from -0.13%/°C to -0.07%/°C when the SIMF grows from 1 to 100 suns, and then increases to -0.10%/°C at 200 suns, mirroring the stochastic response of MJSC to change in SIMF [18]. The figure displays the current-voltage characteristic of each z-matrix at 25°C and 75°C, and for SIMFs of 50 to 200 suns. Using Eqs. (1) and (3), we determined the

MJSC's maximum SI and intensity. Solar concentrators increase the temperature and improve the light absorption of MJSC solar cells [20].

The MJSC's overall efficiency rose nonlinearly with increasing SIMF, reaching a maximum at around 100 SI before gradually declining to a condition of saturation. SCEs decreases from -0.13%/°C to -0.07%/°C when the SIMF grows from 1 to 100 suns, and then increases to -0.10%/°C at 200 suns, mirroring the stochastic response of MJSC to change in SIMF [25]. The figure displays the current-voltage characteristic of each z-matrix at 25°C and 75°C, and for SIMFs of 50 to 200 suns. Using Eqs. (1) and (3), we determined the MJSC's maximum SI and intensity. Solar concentrators raise the temperature and improve the light absorption of MJSC solar cells [26]. The MJSC's overall efficiency rose nonlinearly with increasing SIMF, reaching a maximum at from place to place 100 SI before gradually declining to a condition of saturation.

SCEs decreases from -0.13%/°C to -0.07%/°C when the SIMF grows from 1 to 100 suns, and then increases to -0.10%/°C at 200 suns, mirroring the stochastic response of MJSC to change in SIMF. The figure displays the current-voltage characteristic of each z-matrix at 25°C and 75°C, and for SIMFs of 50 to 200 suns.

4. Summary

Comparing our modelled performance of $Al_xGa_{1-x}As$/InP/Ge MJSCs to that of previous (experimental and simulated) III-V-based MJSC research, we found good agreement. The P_0 and V_{OC} of MJSC decrease (in a linear fashion) with increasing temperature, whereas the SIMF increases (in a logarithmic fashion). The one-diode model approximates SIMF, which is consistent with V_{OC} stochastic behaviour and with high efficiency overall. Reproducing the incoming spectrum light has a cooling effect on the z-matrix level. MJSC composed of $Al_xGa_{1-x}As$/InP/Ge lit at 100 suns and 25°C have the highest efficiency based on substantial parameter expectations that may be beneficial compared to experimental results.

Conflicts of Interest: The authors have not any potential conflicts of interest. To collect and analyses data, to write a manuscript, and to decide whether or not to publish findings.

Acknowledgements: The authors are thanks to Research Lab of Department of Physics, and Central Instrumentation Facilities (CIF), Kalinga University, Naya Raipur (CG) India for the various support.

References

[1]. Sun, Z., Chen, X., He, Y., Li, J., Wang, J., Yan, H., & Zhang, Y. (2022). Toward Efficiency Limits of Crystalline Silicon Solar Cells: Recent Progress in High□ Efficiency Silicon Heterojunction Solar Cells. *Advanced Energy Materials*, *12*(23), 2200015.

[2]. Battaglia, C., Cuevas, A., & De Wolf, S. (2016). High-efficiency crystalline silicon solar cells: status and perspectives. *Energy & Environmental Science*, *9*(5), 1552-1576.

[3]. De Wolf, S., Descoeudres, A., Holman, Z. C., & Ballif, C. (2012). High-efficiency silicon heterojunction solar cells: A review. *green*, *2*(1), 7-24.

[4]. Green, M. A., Zhao, J., Wang, A., & Wenham, S. R. (2001). Progress and outlook for high-efficiency crystalline silicon solar cells. *Solar Energy Materials and Solar Cells*, *65*(1-4), 9-16.

[5]. Verma, A., Diwakar, A. K., & Patel, R. P. (2019). Synthesis and characterization of high-performance solar cell. *International Journal of Scientific Research in Physics and Applied Sciences*, *7*(2), 24-26.

[6]. Kale, A. S., Nemeth, W., Harvey, S. P., Page, M., Young, D. L., Agarwal, S., & Stradins, P. (2018). Effect of silicon oxide thickness on polysilicon based passivated contacts for high-efficiency crystalline silicon solar cells. *Solar Energy Materials and Solar Cells*, *185*, 270-276.

[7]. Blakers, A., Zin, N., McIntosh, K. R., & Fong, K. (2013). High efficiency silicon solar cells. *Energy Procedia*, *33*, 1-10.

[8]. Glunz, S. W., Preu, R., & Biro, D. (2012). Crystalline silicon solar cells: state-of-the-art and future developments. *Comprehensive renewable energy*, *1*, 353-387.

[9]. Ballif, C., Haug, F. J., Boccard, M., Verlinden, P. J., & Hahn, G. (2022). Status and perspectives of crystalline silicon photovoltaics in research and industry. *Nature Reviews Materials*, *7*(8), 597-616.

[10]. Masuko, K., Shigematsu, M., Hashiguchi, T., Fujishima, D., Kai, M., Yoshimura, N., ... & Okamoto, S. (2014). Achievement of more than 25% conversion efficiency with crystalline silicon heterojunction solar cell. *IEEE Journal of Photovoltaics*, *4*(6), 1433-1435.

[11]. Verma, A., Diwakar, A. K., Patel, R. P., & Goswami, P. (2021, September). Characterization CH3NH3PbI3/TiO2 nano-based new generation heterojunction organometallic perovskite solar cell using thin-film technology. In *AIP Conference Proceedings* (Vol. 2369, No. 1, p. 020006). AIP Publishing LLC.

[12]. Zhu, H., Kalkan, A. K., Hou, J., & Fonash, S. J. (1999, March). Applications of AMPS-1D for solar cell simulation. In *AIP Conference Proceedings* (Vol. 462, No. 1, pp. 309-314). American Institute of Physics.

[13]. Rodrigues, E. M. G., Melicio, R., Mendes, V. M. F., & Catalao, J. P. (2011, April). Simulation of a solar cell considering single-diode equivalent circuit model. In *International conference on renewable energies and power quality, Spain* (pp. 13-15).

[14]. Santbergen, R., Meguro, T., Suezaki, T., Koizumi, G., Yamamoto, K., & Zeman, M. (2017). GenPro4 optical model for solar cell simulation and its application to MJSC. *IEEE journal of photovoltaics*, *7*(3), 919-926.

[15]. Mohammed, S. S. (2011). Modeling and Simulation of Photovoltaic module using MATLAB/Simulink. *International Journal of Chemical and Environmental Engineering*, *2*(5).

[16]. Ramos-Hernanz, J. A., Campayo, J. J., Larranaga, J., Zulueta, E., Barambones, O., Motrico, J., ... & Zamora, I. (2012). Two photovoltaic cell simulation models in Matlab/Simulink. *International Journal on Technical and Physical Problems of Engineering,(IJTPE)*, *4*(1), 45-51.

[17]. Patel, J., & Sharma, G. (2013). Modeling and simulation of solar photovoltaic module using matlab/simulink. *International Journal of Research in Engineering and Technology*, *2*(03), 2319-1163.

[18]. Bellia, H., Youcef, R., & Fatima, M. (2014). A detailed modeling of photovoltaic module using MATLAB. *NRIAG journal of astronomy and geophysics*, *3*(1), 53-61.

[19]. Awodugba, A. O., Sanusi, Y. K., & Ajayi, J. O. (2013). Photovoltaic solar cell simulation of shockley diode parameters in matlab. *International Journal of Physical Sciences*, *8*(22), 1193-1200.

[20]. Verma, A., Diwakar, A. K., & Patel, R. P. (2020, March). Characterization of Photovoltaic Property of a CH3NH3Sn1-xGexI3 Lead-Free Perovskite Solar Cell. In *IOP Conference Series: Materials Science and Engineering* (Vol. 798, No. 1, p. 012024). IOP Publishing.

[21]. Zainal, N. A., & Yusoff, A. R. (2016, February). Modelling of photovoltaic module using matlab simulink. In *IOP Conference Series: Materials Science and Engineering* (Vol. 114, No. 1, p. 012137). IOP Publishing.

[22]. Al-Ezzi, A. S., & Ansari, M. N. M. (2022). Photovoltaic Solar Cells: A Review. *Applied System Innovation*, *5*(4), 67.

[23]. Tayeb, A. M., Solyman, A. A., Hassan, M., & el-Ella, T. M. A. (2022). Modeling and simulation of dye-sensitized solar cell: Model verification for different semiconductors and dyes. *Alexandria Engineering Journal*, *61*(12), 9249-9260.

[24]. Needell, D. R., Ilic, O., Bukowsky, C. R., Nett, Z., Xu, L., He, J., ... & Atwater, H. A. (2018). Design criteria for micro-optical tandem luminescent solar concentrators. *IEEE Journal of Photovoltaics*, *8*(6), 1560-1567.

[25]. Nishioka, K., Takamoto, T., Agui, T., Kaneiwa, M., Uraoka, Y., & Fuyuki, T. (2006). Annual output estimation of concentrator photovoltaic systems using high-efficiency InGaP/InGaAs/Ge triple-junction solar cells based on experimental solar cell's characteristics and field-test meteorological data. *Solar Energy Materials and Solar Cells*, *90*(1), 57-67.

[26]. Verma, A. K., Goswami, P., Patel, R. P., Das, S. C., & Verma, A. (2020). Futuristic Energy Source Of CTB (Cs2TiBr6) Thin Films Based Lead-Free Perovskite Solar Cells: Synthesis And Characterization. *Solid State Technology*, *63*(6), 13008-13011.

[27]. Premkumar, M., Chandrasekaran, K., & Sowmya, R. (2020). Mathematical modelling of solar photovoltaic cell/panel/array based on the physical parameters from the manufacturer's datasheet. *International Journal of Renewable energy development*, *9*(1), 7.

[28]. Banik, A., Shrivastava, A., Potdar, R. M., Jain, S. K., Nagpure, S. G., & Soni, M. (2022). Design, modelling, and analysis of novel solar PV system using MATLAB. *Materials today: proceedings*, *51*, 756-763.